PAPER

Peak Cancellation Signal Generation Considering Variance in Signal Power among Transmitter Antennas in PAPR Reduction Method Using Null Space in MIMO Channel for MIMO-OFDM Signals*

Jun SAITO[†], **Nobuhide NONAKA**[††], ***Members***, ***and*** **Kenichi HIGUCHI**[†a)], ***Senior Member***

SUMMARY We propose a novel peak-to-average power ratio (PAPR) reduction method based on a peak cancellation (PC) signal vector that considers the variance in the average signal power among transmitter antennas for massive multiple-input multiple-output (MIMO) orthogonal frequency division multiplexing (OFDM) signals using the null space in a MIMO channel. First, we discuss the conditions under which the PC signal vector achieves a sufficient PAPR reduction effect after its projection onto the null space of the MIMO channel. The discussion reveals that the magnitude of the correlation between the PC signal vector before projection and the transmission signal vector should be as low as possible. Based on this observation and the fact that to reduce the PAPR it is helpful to suppress the variation in the transmission signal power among antennas, which may be enhanced by beamforming (BF), we propose a novel method for generating a PC signal vector. The proposed PC signal vector is designed so that the signal power levels of all the transmitter antennas are limited to be between the maximum and minimum power threshold levels at the target timing. The newly introduced feature in the proposed method, i.e., increasing the signal power to be above the minimum power threshold, contributes to suppressing the transmission signal power variance among antennas and to improving the PAPR reduction capability after projecting the PC signal onto the null space in the MIMO channel. This is because the proposed method decreases the magnitude of the correlation between the PC signal vectors before its projection and the transmission signal vectors. Based on computer simulation results, we show that the PAPR reduction performance of the proposed method is improved compared to that for the conventional method and the proposed method reduces the computational complexity compared to that for the conventional method for achieving the same target PAPR.

key words: *OFDM, PAPR reduction, MIMO, null space, peak cancellation, computational complexity reduction*

1. Introduction

The combination of downlink massive multiple-input multiple-output (MIMO) [1], [2], in which the number of transmitter antennas is very large, and orthogonal frequency division multiplexing (OFDM) signals achieves wide-coverage enhanced mobile broadband communications. However, the peak-to-average power ratio (PAPR) of the OFDM signals is high. In a massive MIMO scenario, the PAPR of the OFDM signals may be further increased due to the variation in the transmission signal power levels among antennas through the beamforming (BF) process. In a massive MIMO environment, a power amplifier with relatively low power consumption needs to be used for each of a large number of transmitter antennas. Therefore, in massive MIMO-OFDM transmission, PAPR reduction is a crucial issue that must be addressed.

In downlink massive MIMO, the number of transmission antennas at a base station is in general much larger than that for receiver antennas at the user terminal. Under this assumption, joint optimization of BF, OFDM modulation, and PAPR reduction was studied in [3]. In [4], a PAPR reduction method was reported in which some of the transmission antennas are exclusively used to reduce the PAPR. In this method, the in-band interference due to the signal for PAPR reduction is eliminated on the receiver side. However, this method decreases the BF gain of the data streams due to the decrease in the number of transmitter antennas used for transmitting the data streams.

In [5]–[16], a PAPR reduction method was discussed that uses the null space in a MIMO channel. This method limits the signal for PAPR reduction transmitted to only the null space in the MIMO channel by applying BF to remove the in-band interference due to the PAPR reduction signal on the receiver side. Since all the transmission antennas are fully utilized for transmission of the data streams, the achievable BF gain of this method is greater than that for the method in [4].

Members of our research group reported a PAPR reduction algorithm based on the peak cancellation (PC) signal in order to reduce the computational complexity in the PAPR reduction method using the null space of a MIMO channel [17]–[19]. This algorithm is referred to as PC with a channel-null constraint (PCCNC). The original idea for the method using the PC signal was reported in [20], [21]. The PC signal is designed so that it has a single dominant peak and satisfies the requirement for out-of-band radiation. By directly adding the PC signal to the transmission signal in the time domain at each transmission antenna, the PAPR of

Manuscript received July 30, 2023.
Manuscript revised March 31, 2024.
Manuscript publicized May 6, 2024.

[†]Graduate School of Science and Technology, Tokyo University of Science, Noda-shi, 278-8510 Japan.
[††]6G-IOWN Promotion Department, NTT DOCOMO, INC., Yokosuka-shi, 239-8536 Japan.

*The material in this paper was presented in part at IEEE Wireless Communications and Networking Conference (WCNC), Glasgow, Scotland, March 2023.

a) E-mail: higuchik@rs.tus.ac.jp

DOI: 10.23919/transcom.2023EBP3125

Copyright © 2024 The Institute of Electronics, Information and Communication Engineers

the transmission signal is suppressed. PCCNC performs PC signal-based PAPR reduction jointly considering all transmission signals for all antennas. Thus, the PC signal is constructed in vector form. The BF vector of the PC signal is set orthogonal to the MIMO channel. In other words, the BF vector of the PC signal is restricted within the null space in the MIMO channel. With this restriction, the interference due to the PC signal that is imparted to the data streams is removed on the receiver side.

The original PCCNC in [17]–[19] first generates the PC signal vector which suppresses all the peak signal components whose power levels are beyond the maximum power threshold in the transmission signals of all transmitter antennas at the target timing. Then, the generated PC signal vector is projected onto the null space in the MIMO channel to calculate the final version of the PC signal vector. However, the PAPR reduction effect of the PC signal vector is degraded to some extent by the projecting operation of the PC signal vector onto the null space in the MIMO channel. Therefore, there is room for improvement in the generation method of the PC signal that suppresses the degradation of the PAPR reduction effect due to projection onto the null space in the MIMO channel. In the following, the original PCCNC in [17] is referred to as conventional PCCNC.

This paper proposes a novel generation method for the PC signal vector for PCCNC. First, we discuss the conditions under which the PC signal vector achieves a sufficient PAPR reduction effect after its projection onto the null space of the MIMO channel. The discussion reveals that the magnitude of the correlation between the PC signal vector before projection onto the null space and the transmission signal vector should be as low as possible. Based on this observation and the fact that it is helpful for PAPR reduction to suppress the variation in the transmission signal power among antennas, which may be enhanced by BF, we propose a novel generation method for the PC signal vector. The proposed PC signal vector is designed so that the signal power levels of all the transmitter antennas are limited to be between the maximum and minimum power threshold levels at the target timing. The newly introduced feature in the proposed method, i.e., increasing the signal power to be above the minimum power threshold, contributes to suppressing the transmission signal power variance among antennas, which directly contributes to the PAPR reduction among antennas. Furthermore, by balancing the PC signal components that reduce the peak signal power and that increase the signal power in the transmission signal vector, the proposed PC signal vector can be uncorrelated with the transmission signal vector. Therefore, the PAPR reduction capability after the projection of the PC signal vector onto the null space in the MIMO channel can be enhanced compared to that for the conventional PCCNC. Based on computer simulation results, we show that the PAPR reduction performance of the proposed PCCNC is improved compared to that of the conventional one and the proposed PCCNC reduces the computational complexity compared to that for the conventional one for achieving the same target PAPR by reducing the required number of iterations in the PCCNC process. We note that the contents of this paper are based on [22], but include enhanced evaluations such as the complexity analysis, evaluation of the complementary cumulative distribution function (CCDF) of the PAPR and throughput, and performance evaluation of the proposed method with various numbers of transmitter antennas.

The remainder of the paper is organized as follows. First, Sect. 2 describes the PCCNC using the conventional PC signal vector generation method, and discusses the conditions for the PC signal vector to achieve sufficient PAPR reduction. Section 3 describes the proposed PC signal vector generation method. Section 4 shows the numerical results based on computer simulations. Finally, Sect. 5 concludes the paper.

2. Conventional PCCNC and Conditions for PC Signal Vector to Achieve Sufficient PAPR Reduction

2.1 Conventional PCCNC

Let us consider MIMO multiplexing where the number of transmitter antennas at the base station is N_{tx} and the number of user terminals each having a single receiver antenna is N_{rx}. We set $N_{\mathrm{tx}} > N_{\mathrm{rx}}$ assuming a downlink massive MIMO scenario. In this paper, we assume that the MIMO channel is not frequency selective for simplicity. The $N_{\mathrm{rx}} \times N_{\mathrm{tx}}$-dimensional channel matrix is denoted as $\mathbf{H}$. Since N_{tx} is greater than N_{rx}, we have $N_{\mathrm{tx}} \times (N_{\mathrm{tx}} - N_{\mathrm{rx}})$-dimensional matrix $\mathbf{K}$ that satisfies $\mathbf{HK} = \mathbf{O}$. All the $N_{\mathrm{tx}} - N_{\mathrm{rx}}$ column vectors in $\mathbf{K}$ are orthonormalized to each other. Matrix $\mathbf{K}$ corresponds to the null space in MIMO channel $\mathbf{H}$.

Hereafter, we explain the conventional PCCNC [17]. Figure 1 shows the block diagram of a base station transmitter with PCCNC. First, the OFDM data stream signal is generated. Then, BF is applied to the OFDM data stream signal to generate the N_{tx}-dimensional transmission signal vector of data streams. After that, PCCNC is processed for a given transmission signal vector in order to reduce the PAPR of the transmission signal vector.

The N_{rx}-dimensional data stream vector at discrete time t ($t = 0, \ldots, F-1$: F is the number of inverse fast Fourier transform (IFFT) points in OFDM signal generation) is denoted as $\mathbf{s}[t]$. The $N_{\mathrm{tx}} \times N_{\mathrm{rx}}$-dimensional BF matrix, $\mathbf{M}$, is multiplied to $\mathbf{s}[t]$ to generate the N_{tx}-dimensional time-domain transmission signal vector before PAPR reduction, $\mathbf{x}[t]$. Vector $\mathbf{x}[t]$ is represented as

$$\mathbf{x}[t] = \begin{bmatrix} x_1[t] & \cdots & x_{N_{\mathrm{tx}}}[t] \end{bmatrix}^T = \mathbf{M}\mathbf{s}[t], \tag{1}$$

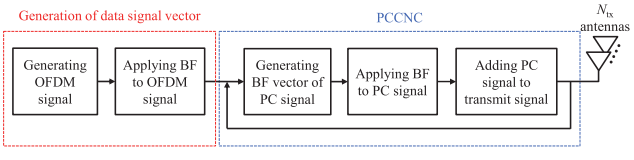

Fig. 1 Block diagram of base station transmitter with PCCNC.

where $x_n[t]$ is the n-th element of $\mathbf{x}[t]$, which is transmitted from transmitter antenna n.

PCCNC reduces the PAPR by iteratively repeating the direct addition of the PC signal vectors to transmission signal vector $\mathbf{x}[t]$. The PC signal vector is generated by multiplying BF vector, $\mathbf{m}_{\mathrm{pc}}$, which is directed to the null space in the MIMO channel, to the time-shifted version of basic time-domain signal, $b[t]$, which is a sinc function whose dominant peak amplitude at $t = 0$ is set to 1 and whose bandwidth is equal to the signal transmission bandwidth.

The time-domain transmission signal vector at the j-th iteration of the PCCNC process is denoted as $\mathbf{x}^{(j)}[t] = \left[x_1^{(j)}[t] \quad \cdots \quad x_{N_{\mathrm{tx}}}^{(j)}[t]\right]^T$. We assume $\mathbf{x}^{(1)}[t] = \mathbf{x}[t]$ as the initial setting. At the j-th iteration, PCCNC tries to reduce the PAPR observed in $\mathbf{x}^{(j)}[t]$ at target time index $\tau^{(j)}$. Target time index $\tau^{(j)}$ is determined based on the peak observation in $\mathbf{x}^{(j)}[t]$. More specifically, $\tau^{(j)}$ is set to the time index where $x_n^{(j)}[t]$ has the maximum amplitude for all $n = 1, \ldots, N_{\mathrm{tx}}$ and $t = 0, \ldots, F-1$. In the j-th iteration of the conventional PCCNC, the PC signal vector, $\mathbf{c}^{(j)}[t]$, which is represented in the form of (2), is added to $\mathbf{x}^{(j)}[t]$.

$$\mathbf{c}^{(j)}[t] = \mathbf{m}_{\mathrm{pc}}^{(j)} b\left[t - \tau^{(j)}\right]. \tag{2}$$

$$\mathbf{x}^{(j+1)}[t] = \mathbf{x}^{(j)}[t] + \mathbf{c}^{(j)}[t]. \tag{3}$$

The purpose of $\mathbf{c}^{(j)}[t]$ in the conventional PCCNC is to suppress the peak signal observed in $\mathbf{x}^{(j)}[\boldsymbol{\tau}^{(j)}]$ using the dominant peak signal portion of $b[0]$.

An important component of $\mathbf{c}^{(j)}[t]$ is its BF vector, $m_{\mathrm{pc}}^{(j)}$, and investigating its generation method is the purpose of this paper. The N_{tx}-dimensional vector, $\mathbf{m}_{\mathrm{pc}}^{(j)}$, should lie within null space $\mathbf{K}$ in the MIMO channel. PC signal vector $\mathbf{c}^{(j)}[t]$ is generated by multiplying $\mathbf{m}_{\mathrm{pc}}^{(j)}$ to the $\tau^{(j)}$-time-shifted version of $b[t]$. Thus, PC signal vector $\mathbf{c}^{(j)}[t]$ meets the requirement of out-of-band radiation and does not interfere with the data streams. This is because the PC signal is transmitted to only the null space in the given MIMO channel and does not appear on the receiver side. In generating $\mathbf{m}_{\mathrm{pc}}^{(j)}$, the first step is to find BF vector $\tilde{\mathbf{m}}_{\mathrm{pc}}^{(j)}$ of the PC signal vectors that are desirable from the viewpoint of PAPR suppression. Next, $\mathbf{m}_{\mathrm{pc}}^{(j)}$ is generated by projecting $\tilde{\mathbf{m}}_{\mathrm{pc}}^{(j)}$ onto null space $\mathbf{K}$ in the MIMO channel.

Figure 2 shows the conventional method for PC signal generation described in [17]. In [17], $\tilde{\mathbf{m}}_{\mathrm{pc}}^{(j)}$ is generated using the following formula.

$$\tilde{\mathbf{m}}_{\mathrm{pc}}^{(j)} = \left[\tilde{m}_{\mathrm{pc},1}^{(j)} \quad \cdots \quad \tilde{m}_{\mathrm{pc},N_{\mathrm{tx}}}^{(j)}\right]^T,$$

where

$$\tilde{m}_{\mathrm{pc},n}^{(j)} = \begin{cases} \sqrt{P_{\mathrm{U}}} e^{j\theta_n^{(j)}[\tau^{(j)}]} - x_n^{(j)}\left[\tau^{(j)}\right], & \left|x_n^{(j)}\left[\tau^{(j)}\right]\right|^2 > P_{\mathrm{U}} \\ 0, & \text{Otherwise} \end{cases}. \tag{4}$$

Here, P_{U} is the maximum power threshold and $\theta_n^{(j)}[\tau^{(j)}]$ is the phase of $x_n^{(j)}[\tau^{(j)}]$. Vector $\tilde{\mathbf{m}}_{\mathrm{pc}}^{(j)}$ is the ideal peak reduction vector in the sense that if $\tilde{\mathbf{m}}_{\mathrm{pc}}^{(j)}$ is used as $\mathbf{m}_{\mathrm{pc}}^{(j)}$ in (2), the transmission signal power levels for all N_{tx} antennas at time $\tau^{(j)}$ (thus, $|x_n^{(j)}[\tau^{(j)}]|^2$ for all n) can simultaneously be suppressed to equal to or lower than maximum power threshold P_{U} as shown in Fig. 2.

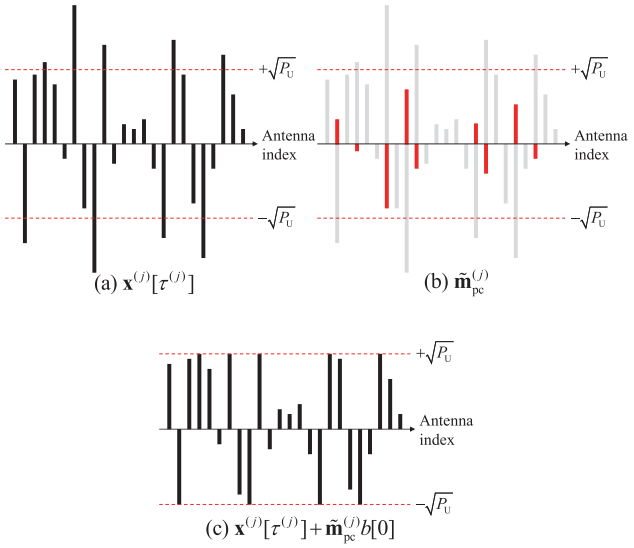

Fig. 2 Conventional PC signal vector.

However, $\tilde{\mathbf{m}}_{\mathrm{pc}}^{(j)}$ has an element that is orthogonal to the null space in the MIMO channel, which leads to interference to the data streams. Therefore, $\tilde{\mathbf{m}}_{\mathrm{pc}}^{(j)}$ is projected onto null space $\mathbf{K}$ in the MIMO channel to obtain $\mathbf{m}_{\mathrm{pc}}^{(j)}$ in (2).

$$\mathbf{m}_{\mathrm{pc}}^{(j)} = \mathbf{K}\mathbf{K}^H \tilde{\mathbf{m}}_{\mathrm{pc}}^{(j)}. \tag{5}$$

2.2 Discussions on Conditions for PC Signal Vector to Achieve Sufficient PAPR Reduction Effect

The conventional method for generating the BF vector of the PC signal before projection $\tilde{\mathbf{m}}_{\mathrm{pc}}^{(j)}$ in [17] is based on a standard approach in PAPR reduction, i.e., clipping of the high peak power components. However, as revealed below, there is room for improvement in terms of the PAPR reduction effect after its projection onto the null space $\mathbf{K}$ in the MIMO channel. Hereafter, we analyze the impact of the projection of the PC signal vector onto the null space in the MIMO channel on the PAPR reduction capability. For simplicity of notation, we consider the $j = 1$-st PAPR reduction process of PCCNC and denote $\mathbf{x}^{(1)}[t] = \mathbf{x}[t]$, $\tilde{\mathbf{m}}_{\mathrm{pc}}^{(1)}$, and $\mathbf{m}_{\mathrm{pc}}^{(1)}$ by $\mathbf{x}$, $\tilde{\mathbf{m}}_{\mathrm{pc}}$, and $\mathbf{m}_{\mathrm{pc}}$, respectively.

PCCNC must have a large correlation between $\tilde{\mathbf{m}}_{\mathrm{pc}}$ and $\mathbf{m}_{\mathrm{pc}}$, which is the projection of $\tilde{\mathbf{m}}_{\mathrm{pc}}$ onto the null space $\mathbf{K}$ in the MIMO channel, in order to obtain a sufficient PAPR reduction effect, assuming that $\tilde{\mathbf{m}}_{\mathrm{pc}}$ is designed to achieve a good PAPR reduction capability. The correlation between $\mathbf{m}_{\mathrm{pc}}$ and $\tilde{\mathbf{m}}_{\mathrm{pc}}$, $R(\mathbf{m}_{\mathrm{pc}})$, is represented as

$$R\left(\mathbf{m}_{\mathrm{pc}}\right) = \frac{\tilde{\mathbf{m}}_{\mathrm{pc}}^H \mathbf{m}_{\mathrm{pc}}}{\left\|\tilde{\mathbf{m}}_{\mathrm{pc}}\right\| \cdot \left\|\mathbf{m}_{\mathrm{pc}}\right\|} = \frac{\tilde{\mathbf{m}}_{\mathrm{pc}}^H \mathbf{K}\mathbf{K}^H \tilde{\mathbf{m}}_{\mathrm{pc}}}{\left\|\tilde{\mathbf{m}}_{\mathrm{pc}}\right\| \cdot \left\|\mathbf{m}_{\mathrm{pc}}\right\|} = \frac{\left\|\mathbf{K}^H \tilde{\mathbf{m}}_{\mathrm{pc}}\right\|^2}{\left\|\tilde{\mathbf{m}}_{\mathrm{pc}}\right\| \cdot \left\|\mathbf{m}_{\mathrm{pc}}\right\|}. \tag{6}$$

From (6), $R(\mathbf{m}_{\mathrm{pc}})$ is always a non-negative real number and is determined by $\|\mathbf{K}^H\tilde{\mathbf{m}}_{\mathrm{pc}}\|$. Therefore, it is important to prevent $\mathbf{K}$ and $\tilde{\mathbf{m}}_{\mathrm{pc}}$ from being orthogonal as much as possible.

Clearly, the BF vector of the PC signal before projection $\tilde{\mathbf{m}}_{\mathrm{pc}}$ is generated based on given transmission signal vector $\mathbf{x}$. BF matrix $\mathbf{M}$ for data streams to generate $\mathbf{x}$ as $\mathbf{x} = \mathbf{M}\mathbf{s}$ is orthogonal to null space $\mathbf{K}$ in the MIMO channel. This is because $\mathbf{M}$ aims to send data stream $\mathbf{s}$ to the destination user terminal regardless of the BF criteria such as zero forcing (ZF), minimum mean squared error (MMSE), or an eigenmode MIMO-based criterion. Therefore,

$$\mathbf{K}^H\mathbf{x} = \mathbf{K}^H\mathbf{M}\mathbf{s} = \mathbf{0}. \tag{7}$$

Thus, transmission signal vector $\mathbf{x}$ is orthogonal to $\mathbf{K}$.

The conventional method generates $\tilde{\mathbf{m}}_{\mathrm{pc}}$ so that it eliminates the signal elements above maximum power threshold P_{U}. Therefore, $\tilde{\mathbf{m}}_{\mathrm{pc}}$ and transmission signal vector $\mathbf{x}$ have a negative correlation as illustrated in Fig. 2. If we assume the extreme condition of $P_{\mathrm{U}} = 0$, $\tilde{\mathbf{m}}_{\mathrm{pc}}$ becomes $-\mathbf{x}$ and $R(\mathbf{m}_{\mathrm{pc}})$ becomes

$$R\left(\mathbf{m}_{\mathrm{pc}}\right) = \frac{\left\|\mathbf{K}^H\tilde{\mathbf{m}}_{\mathrm{pc}}\right\|^2}{\left\|\tilde{\mathbf{m}}_{\mathrm{pc}}\right\| \cdot \left\|\mathbf{m}_{\mathrm{pc}}\right\|} = \frac{\left\|-\mathbf{K}^H\mathbf{x}\right\|^2}{\left\|\tilde{\mathbf{m}}_{\mathrm{pc}}\right\| \cdot \left\|\mathbf{m}_{\mathrm{pc}}\right\|} = 0. \tag{8}$$

This means that after projecting $\tilde{\mathbf{m}}_{\mathrm{pc}}$ onto null space $\mathbf{K}$ in the given MIMO channel, $\mathbf{m}_{\mathrm{pc}}$ becomes $\mathbf{0}$ and no PAPR reduction is achieved.

Based on the above discussion, the BF vector of the PC signal before projection, $\tilde{\mathbf{m}}_{\mathrm{pc}}$, should be uncorrelated with transmission signal vector $\mathbf{x}$ as much as possible. Then, null space $\mathbf{K}$ and $\tilde{\mathbf{m}}_{\mathrm{pc}}$ will no longer be orthogonal, so $R(\mathbf{m}_{\mathrm{pc}})$ will increase and the PAPR reduction effect can be expected to increase.

3. Proposed PC Signal Vector Generation Method

Based on the discussion in Sect. 2, we propose a novel method for generating the PC signal vector, more specifically, a new method for generating $\tilde{\mathbf{m}}_{\mathrm{pc}}^{(j)}$.

Conventional $\tilde{\mathbf{m}}_{\mathrm{pc}}^{(j)}$ calculated using (4) has a negative correlation with transmission signal vector $\mathbf{x}^{(j)}[\tau^{(j)}]$. If the magnitude of the correlation between $\tilde{\mathbf{m}}_{\mathrm{pc}}^{(j)}$ and $\mathbf{x}^{(j)}[\tau^{(j)}]$ can be decreased by adding a component that has a positive correlation with transmission signal vector $\mathbf{x}^{(j)}[\tau^{(j)}]$ with respect to conventional $\tilde{\mathbf{m}}_{\mathrm{pc}}^{(j)}$, the PAPR reduction capability after projecting $\tilde{\mathbf{m}}_{\mathrm{pc}}^{(j)}$ onto the null space in the MIMO channel can be enhanced.

On the other hand, the PAPR in MIMO transmission also increases due to the variance in the average transmission signal power among transmission antennas due to BF. Here, if a signal component that increases the transmission signal power for an antenna with a low transmission signal power is included in $\tilde{\mathbf{m}}_{\mathrm{pc}}^{(j)}$ in order to decrease the variance of the average transmission signal power levels among transmission antennas, such a signal component can be expected to have a positive correlation with $\mathbf{x}^{(j)}[\tau^{(j)}]$.

Based on the above analysis, we propose a new generation method for the PC signal vector. In the proposed method, the BF vector of the PC signal before projection, $\tilde{\mathbf{m}}_{\mathrm{pc}}^{(j)}$, is designed so that the signal power levels of all the transmission antennas at the target timing are restricted to be between the maximum and minimum power threshold levels. In the proposed method, we define the minimum power threshold, P_{L}, in addition to the maximum power threshold P_{U}, where P_{U} is greater than P_{L}. Proposed $\tilde{\mathbf{m}}_{\mathrm{pc}}^{(j)}$ is represented as

$$\tilde{\mathbf{m}}_{\mathrm{pc}}^{(j)} = \begin{bmatrix} \tilde{m}_{\mathrm{pc},1}^{(j)} & \cdots & \tilde{m}_{\mathrm{pc},N_{\mathrm{tx}}}^{(j)} \end{bmatrix}^T,$$

where

$$\tilde{m}_{\mathrm{pc},n}^{(j)} = \begin{cases} \sqrt{P_{\mathrm{U}}}e^{j\theta_n^{(j)}[\tau^{(j)}]} - x_n^{(j)}\left[\tau^{(j)}\right], & \left|x_n^{(j)}\left[\tau^{(j)}\right]\right|^2 > P_{\mathrm{U}} \\ \sqrt{P_{\mathrm{L}}}e^{j\theta_n^{(j)}[\tau^{(j)}]} - x_n^{(j)}\left[\tau^{(j)}\right], & \left|x_n^{(j)}\left[\tau^{(j)}\right]\right|^2 < P_{\mathrm{L}} \\ 0, & \text{Otherwise} \end{cases}. \tag{9}$$

Figure 3 shows the proposed PC signal generation. The first component of $\tilde{\mathbf{m}}_{\mathrm{pc}}^{(j)}$ shown in the first line in (9), which is shown in red in Fig. 3(b), is the same as in the conventional method using (4). With this component, the transmission signal power levels for all N_{tx} antennas at time $\tau^{(j)}$ (thus, $|x_n^{(j)}[\tau^{(j)}]|^2$ for all n) can simultaneously be set equal to or lower than maximum power threshold P_{U}. This component has a negative correlation with $\mathbf{x}^{(j)}[\tau^{(j)}]$.

The second component of $\tilde{\mathbf{m}}_{\mathrm{pc}}^{(j)}$ shown in the second line in (9), which is shown in green in Fig. 3(b), is newly introduced in the proposed method. With this component, the transmission signal power levels for all N_{tx} antennas at time $\tau^{(j)}$ (thus, $|x_n^{(j)}[\tau^{(j)}]|^2$ for all n) can simultaneously be set equal to or higher than minimum power threshold P_{L}. This component has a positive correlation with $\mathbf{x}^{(j)}[\tau^{(j)}]$.

By balancing the two components, the correlation between $\tilde{\mathbf{m}}_{\mathrm{pc}}^{(j)}$ and $\mathbf{x}^{(j)}[\tau^{(j)}]$ can be close to 0. As a consequence,

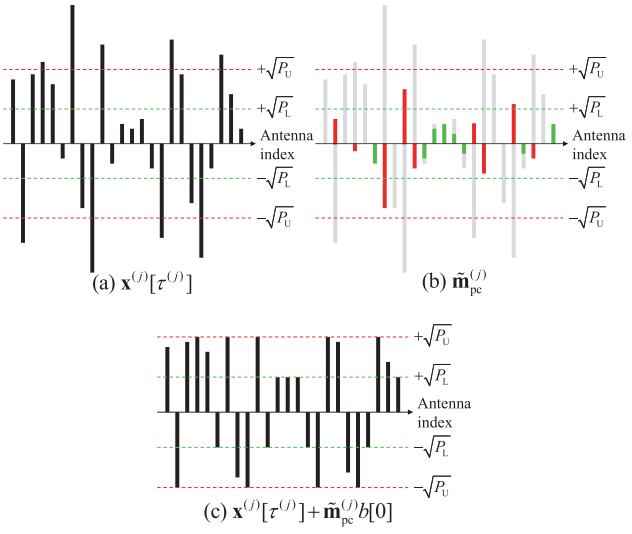

Fig. 3 Proposed PC signal vector.

$R\left(\mathbf{m}_{\mathrm{pc}}\right) = \|\mathbf{K}^H\tilde{\mathbf{m}}_{\mathrm{pc}}\|^2/\|\tilde{\mathbf{m}}_{\mathrm{pc}}\|\cdot\|\mathbf{m}_{\mathrm{pc}}\|$ can be increased, and the PAPR reduction effect after projection onto the null space in the MIMO channel can be enhanced. The proposed method also reduces the PAPR by directly reducing the variance in the average transmission signal power levels among transmitter antennas.

In the proposed method, the final PC signal vector, $\mathbf{m}_{\mathrm{pc}}^{(j)}$, is generated by applying the null restriction using (5) to the generated $\tilde{\mathbf{m}}_{\mathrm{pc}}^{(j)}$, which is the same as in the conventional PCCNC. Since the proposed method only adds the process of the minimum power threshold to the conventional method, the computational cost such as the required number of real multiplications per iteration for the proposed method is approximately the same as in the conventional method.

4. Numerical Results

The performance of the proposed PCCNC is evaluated based on computer simulations and compared to the conventional PCCNC [17]. The number of transmitter antennas, N_{tx}, is parameterized. The number of receiving user terminals, N_{rx}, is set to 4. The ZF-based BF is applied to actualize multiuser MIMO. The number of subcarriers in the OFDM signal is 64. The number of FFT/IFFT points is set to 256, which corresponds to 4-times oversampling in the time domain in order to measure satisfactorily accurate PAPR levels [23]. For general evaluation, we assume that the signal constellation of each subcarrier follows an independent standard complex Gaussian distribution. Flat Rayleigh fading is assumed as the channel model, which is independent between transmitter antennas and between receiving users. The signal-to-noise ratio (SNR) is set to 20 dB. In the proposed PCCNC and the conventional PCCNC, we assume that after J iterations, per-antenna PC-based PAPR reduction (PAPC) [20], [21] is applied with J_{add} iterations in order to achieve a lower PAPR at the cost of reduced throughput. Maximum power threshold P_{U} and minimum power threshold P_{L} are defined as the signal power threshold normalized by the signal power per antenna averaged over the channel realizations. The PAPR is defined as the ratio of the peak signal power to the average signal power across all the transmitter antennas per OFDM symbol. The sum throughput of N_{rx} streams (users) is measured based on the Shannon formula taking into account the Bussgang's theorem [24].

Figure 4 shows the average $R(\mathbf{m}_{\mathrm{pc}})$ as a function of P_{L} in the proposed PCCNC. The number of transmitter antennas, N_{tx}, is set to 100. Threshold P_{U} is 6 dB and iterations of the proposed PCCNC, J, is parameterized from 1 to 20. Overall, the average $R(\mathbf{m}_{\mathrm{pc}})$ increases by setting P_{L} to be larger than P_{L} of -100 dB, which corresponds to the conventional PCCNC. This suggests that the degradation in the PAPR reduction effect accompanying the projection processing onto the null space in the MIMO channel of the PC signal vector can be alleviated using an appropriate P_{L} in the proposed PCCNC compared to that in the conventional PCCNC. As J is increased, the P_{L} that maximizes the average $R(\mathbf{m}_{\mathrm{pc}})$ is decreased. This is because the transmission signal

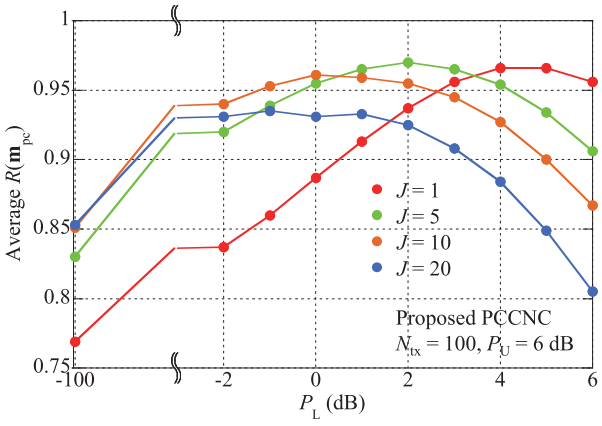

Fig. 4 Average $R(\mathbf{m}_{\mathrm{pc}})$ as a function of P_{L}.

vector at J-th iteration $\mathbf{x}^{(J)}[t]$ contains the PC signal vectors that are added at up to $J-1$ iterations, which increases the correlation between null space $\mathbf{K}$ in the MIMO channel and $\mathbf{x}^{(J)}[t]$. Therefore, the necessity for the PC signal components to increase the power level of the signal below minimum power threshold P_{L} that has a positive correlation with $\mathbf{x}[t]$ decreases, and a lower P_{L} is considered to be optimum from the viewpoint of maximizing the average $R(\mathbf{m}_{\mathrm{pc}})$.

To estimate the degree of improvement in the PAPR reduction effect per added PC signal in the proposed method, we evaluated the peak power reduction ratio, G_{peak}, which is defined as

$$G_{\mathrm{peak}} = \left(\frac{A_{\mathrm{after}} - \sqrt{P_{\mathrm{U}}}}{A_{\mathrm{before}} - \sqrt{P_{\mathrm{U}}}}\right)^2. \tag{10}$$

Here, A_{before} and A_{after} are the amplitudes of the peak signal component before and after addition of the PC signal at the J-th iteration, respectively. Ratio G_{peak} is a measure of how much the addition of the PC signal reduces the signal power above maximum power threshold P_{U}. Figure 5 shows the average G_{peak} as a function of P_{L} for the proposed PCCNC. Term N_{tx} is set to 100. Threshold P_{U} is 6 dB and J is parameterized. The average G_{peak} is decreased by appropriately setting the P_{L} levels for the respective J. From Figs. 4 and 5, we see that the best P_{L} level that maximizes the average $R(\mathbf{m}_{\mathrm{pc}})$ coincides with the P_{L} level that minimizes the average G_{peak} for the respective J. This confirms the validity of the analysis regarding the conditions for the PC signal vector to achieve a sufficient PAPR reduction capability after projection onto the null space in the MIMO channel in this paper.

In the proposed PCCNC, another factor that further reduces the PAPR compared to the conventional PCCNC is the reduction of the variance in the average transmission signal power among transmitter antennas after addition of the PC signal. To assess this effect, the reduction rate of the variance in the average transmission signal power among transmission antennas, G_{ant}, is evaluated. Term G_{ant} is defined as

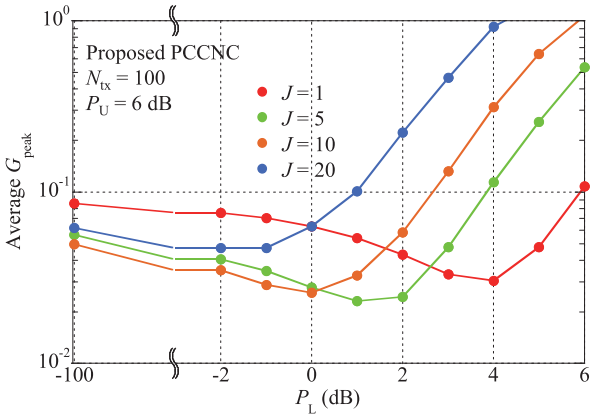

Fig. 5 Average G_{peak} as a function of P_{L}.

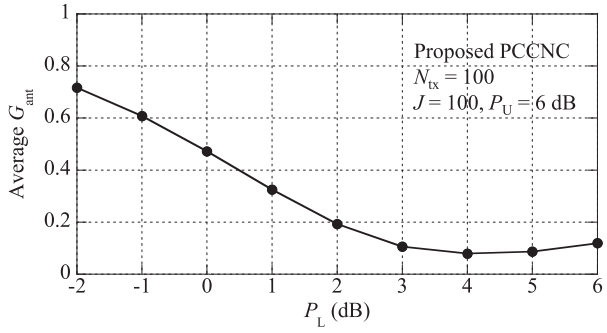

Fig. 6 Average G_{ant} as a function of P_{L}.

$$G_{\text{ant}} = \frac{\text{Var}\left[\overline{P}_n^{\text{prop.}}\right]}{\text{Var}\left[\overline{P}_n^{\text{conv.}}\right]}. \tag{11}$$

Here, $\text{Var}\left[\overline{P}_n^{\text{prop.}}\right]$ and $\text{Var}\left[\overline{P}_n^{\text{conv.}}\right]$ are the variance in the average transmission signal power among N_{tx} transmitter antennas when the proposed PCCNC and the conventional PCCNC are used, respectively. Figure 6 shows the average G_{ant} as a function of P_{L}. Term N_{tx} is set to 100. Number of iterations J is set to 100 and P_{U} is 6 dB. From Fig. 6, the variance in the average transmission signal power among transmitter antennas is suppressed by using the proposed PCCNC with an appropriate setting for P_{L}.

Figures 7 and 8 show the CCDF of the PAPR and throughput, respectively. The proposed PCCNC with P_{L} as a parameter and the conventional PCCNC are tested. Term N_{tx} is set to 100. Maximum power threshold P_{U} and J are set to 6 dB and 100, respectively. Term J_{add} is set to 60. Based on Fig. 7, the PAPR distribution of the proposed PCCNC is improved as P_{L} is set larger. This is because the proposed PCCNC increases the PAPR reduction effect after the projection of the PC signal onto the null space in the MIMO channel and reduces the average transmission power variance among the transmitter antennas. From Fig. 8, the throughput of the proposed PCCNC at the CCDF of 0.5 is most improved when P_{L} is set between −2 dB and 2 dB.

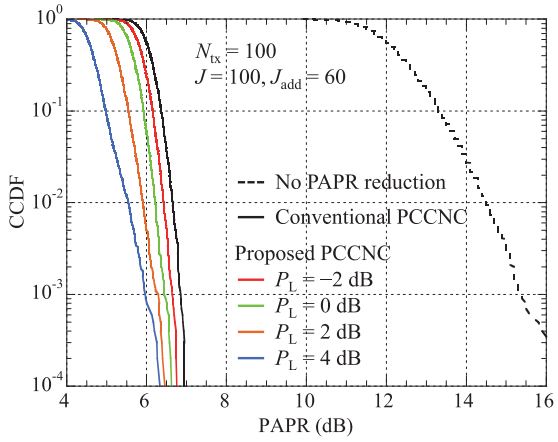

Fig. 7 CCDF of PAPR.

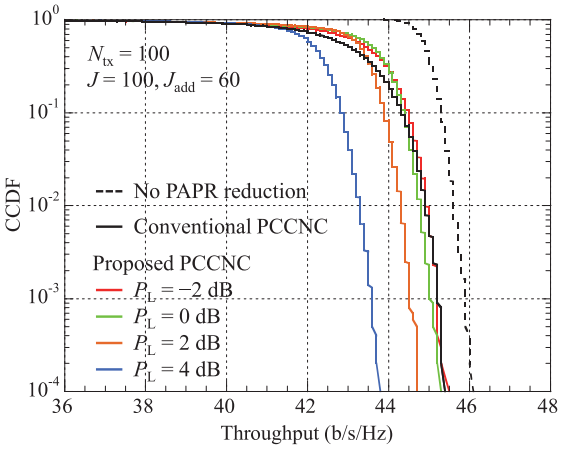

Fig. 8 CCDF of throughput.

With this P_{L} setting, the throughput with the proposed PCCNC is higher than that with the conventional PCCNC. This is because the proposed PCCNC can sufficiently suppress the peak power, and the subsequent PAPC does not need to generate much of a PC signal to suppress the residual peaks. Therefore, in the proposed method, interference caused by the PC signal of PAPC can be decreased compared to that for the conventional PCCNC. On the other hand, the throughput of the proposed PCCNC with the relatively high P_{L} value of 4 dB is degraded. This is because the transmission power for data signal transmission is reduced since a large fraction of the total transmission power is consumed for the PC signal transmission to increase the transmission power of the signal component whose power is below minimum power threshold P_{L}.

Figure 9 shows the average throughput as a function of the average PAPR. The proposed PCCNC with P_{L} as a parameter and the conventional PCCNC are tested. Term N_{tx} is set to 100. The numbers of iterations of PCCNC and PAPC, J and J_{add}, are set to 100 and 60, respectively, for both proposed and conventional PCCNCs. The relationship between the average PAPR and the average throughput is varied by changing P_{U} for the respective methods. Figure 9

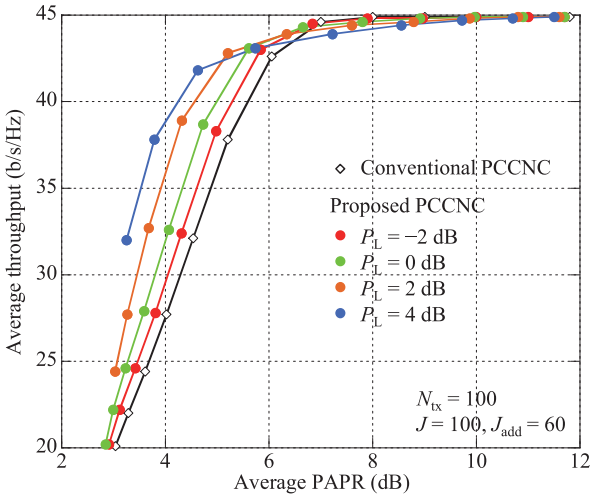

Fig. 9 Average throughput as a function of average PAPR.

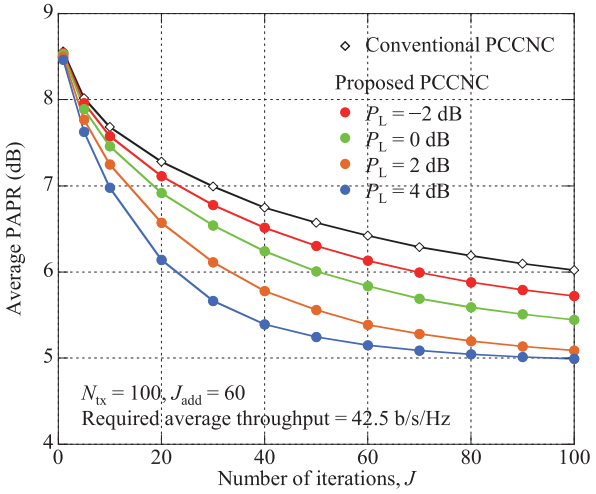

Fig. 10 Average PAPR for required average throughput as a function of J.

shows that the proposed method increases the throughput compared to that for the conventional PCCNC for the same required PAPR level, especially when the required PAPR is small. This is because the proposed method achieves a sufficient PAPR reduction more efficiently using the PC signal directed to the null space in the MIMO channel by decorrelating the PC signal and transmission data signal. Furthermore, the proposed method suppresses the variance in the average transmission signal power among transmitter antennas, which directly contributes to the reduction in PAPR.

Figure 10 shows the average PAPR for the required average throughput of 42.5 b/s/Hz as a function of the number of iterations, J. The proposed PCCNC with P_L as a parameter and the conventional PCCNC are tested. Term N_{tx} is set to 100. The numbers of iterations for PAPC, J_{add}, is fixed at 60 for all methods. For each J of the respective methods, P_U is adjusted so that the required average throughput of 42.5 b/s/Hz is satisfied. The proposed PCCNC decreases the average PAPR compared to that for the conventional PCCNC for the same J. This is because the proposed PCCNC achieves a superior PAPR reduction effect by decorrelating the PC signal and transmission data signal, which also contributes to reducing the variance in the average transmission signal power among the transmitter antennas. As mentioned in Sect. 3, the computational cost such as the required number of real multiplications per iteration for the proposed PCCNC is approximately the same as that for the conventional one, since the proposed PCCNC only adds the process of the minimum power threshold to the conventional one. Therefore, the reduction in the required number of iterations for achieving the same PAPR shown in Fig. 10 indicates that the proposed PCCNC reduces the computational cost compared to the previous PCCNC for achieving the same PAPR.

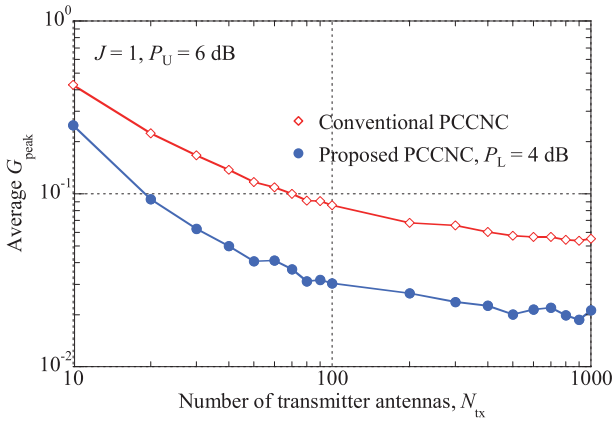

Fig. 11 Average G_{peak} as a function of N_{tx}.

In the following, performance evaluations with various N_{tx} are presented to assess the impact of the dimensions of the null space in the MIMO channel on the performance of the proposed method. Figure 11 shows the average G_{peak} as a function of N_{tx}. Terms J and P_U are set to 1 and 6 dB, respectively. The proposed PCCNC with the P_L value of 4 dB and conventional PCCNC are tested. Both the proposed and conventional PCCNCs achieve lower average G_{peak} as N_{tx} is increased, thanks to the increased dimensions of the null space in the MIMO channel. The proposed PCCNC achieves a lower G_{peak} than the conventional PCCNC regardless of the N_{tx} value.

Figure 12 shows the average G_{ant} as a function of N_{tx}. Term J is set to 100. Thresholds P_U and P_L are set to 6 dB and 4 dB, respectively. The average G_{ant} is reduced as N_{tx} is increased. Thus, the performance gain by using the proposed PCCNC in terms of the reduction in the variance in the average transmission signal power among transmitter antennas is increased as the dimensions of the null space in the MIMO channel increases.

Figure 13 shows the average throughput as a function of the average PAPR. Term N_{tx} is parameterized from 20 to 1000. The proposed PCCNC with the P_L value of 4 dB and conventional PCCNC are tested. The relationship between the average PAPR and the average throughput is varied by changing P_U for the respective methods. Terms J and J_{add}

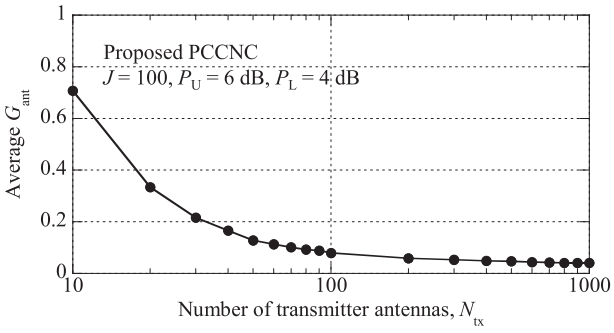

Fig. 12 Average G_{ant} as a function of N_{tx}.

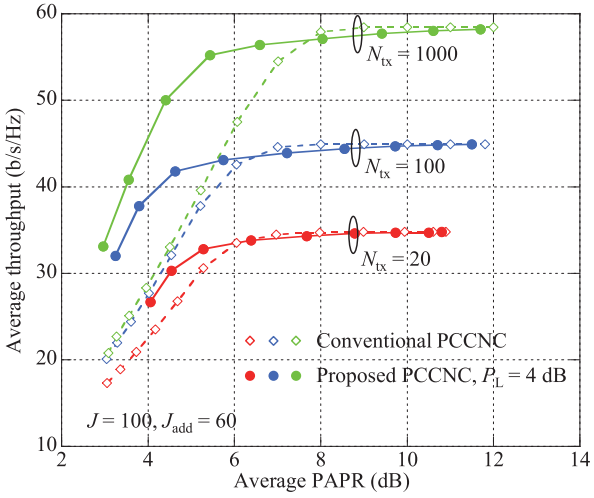

Fig. 13 Average throughput as a function of average PAPR for various N_{tx}.

are set to 100 and 60, respectively. Figure 13 shows that the proposed PCCNC increases the throughput compared to that for the conventional PCCNC for the same required PAPR level, especially when the required PAPR is small. The throughput gain by using the PCCNC compared to that for the conventional one is increased as N_{tx} is increased. This confirms that the proposed PCCNC is effective especially when the dimensions of the null space in the MIMO channel are large.

Figure 14 shows the average PAPR for the required average throughput as a function of N_{tx}. The required average throughput for each N_{tx} is defined as the 95% value of the achievable throughput when no PAPR reduction is performed. The proposed PCCNC with the P_L value of 4 dB and conventional PCCNC are tested. Terms J and J_{add} are set to 100 and 60, respectively, for both methods. The proposed PCCNC achieves a lower PAPR than that for the conventional one for all N_{tx}. The conventional PCCNC increases the PAPR as N_{tx} is increased. This is mainly due to the increased variance in the average transmission signal power among the transmitter antennas. On the other hand, the proposed PCCNC significantly reduces the PAPR by maintaining the PAPR reduction capability after projecting the PC signal vector onto the channel null and suppressing the variance in the average transmission signal power among the transmitter antennas when N_{tx} is very large.

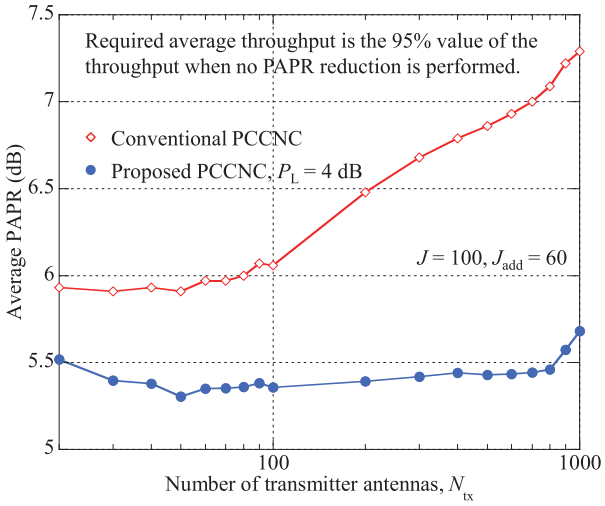

Fig. 14 Average PAPR for required average throughput as a function of N_{tx}.

5. Conclusion

This paper proposed a new generation method for the PC signal vector, which has a component that increases the transmission power of the transmission signal so that the transmission signal power levels for all transmitter antennas at the target timing can simultaneously be set equal to or higher than the minimum power threshold. This is completely different from the conventional standard concept of PAPR reduction, i.e., the clipping of the high peak power components. This new idea decorrelates the PC signal vector and transmit data signal vector, and this enables more PC signal components for PAPR reduction to be emitted to the null space of the given MIMO channel. Furthermore, the variance in the average transmission signal power levels among antennas, which is one cause for the PAPR increase in MIMO transmission with BF, can be suppressed. As a result, the proposed method achieves a greater PAPR reduction effect than the conventional method. This paper assumes a frequency nonselective channel. The extension of the proposed method to accommodate a frequency selective channel is possible by utilizing the approach in [18] for example. Detailed investigation on extending the proposed method to accommodate a frequency selective channel as well as investigating a more power efficient construction for the PC signal vector are left for future study.

References

[1] T.L. Marzetta, "Noncooperative cellular wireless with unlimited numbers of base station antennas," IEEE Trans. Wireless Commun., vol.9, no.11, pp.3590–3600, Nov. 2010.
[2] H. Papadopoulos, C. Wang, O. Bursalioglu, X. Hou, and Y. Kishiyama, "Massive MIMO technologies and challenges towards 5G," IEICE Trans. Commun., vol.E99-B, no.3, pp.602–621, March

2016.
[3] C. Studer and E.G. Larsson, "PAR-aware large-scale multi-user MIMO-OFDM downlink," IEEE J. Sel. Areas Commun., vol.31, no.2, pp.303–313, Feb. 2013.
[4] H. Prabhu, O. Edfors, J. Rodrigues, L. Liu, and F. Rusek, "A low-complex peak-to-average power reduction scheme for OFDM based massive MIMO systems," Proc. ISCCSP2014, Athens, Greece, May 2014.
[5] M. Iwasaki and K. Higuchi, "Clipping and filtering-based PAPR reduction method for precoded OFDM-MIMO signals," Proc. IEEE VTC2010-Spring, Taipei, Taiwan, May 2010.
[6] Y. Sato, M. Iwasaki, S. Inoue, and K. Higuchi, "Clipping and filtering-based adaptive PAPR reduction method for precoded OFDM-MIMO signals," IEICE Trans. Commun., vol.E96-B, no.9, pp.2270–2280, Sept. 2013.
[7] S. Inoue, T. Kawamura, and K. Higuchi, "Throughput/ACLR performance of CF-based adaptive PAPR reduction method for eigenmode MIMO-OFDM signals with AMC," IEICE Trans. Commun., vol.E96-B, no.9, pp.2293–2300, Sept. 2013.
[8] R. Kimura, Y. Tajika, and K. Higuchi, "CF-based adaptive PAPR reduction method for block diagonalization-based multiuser MIMO-OFDM signals," Proc. IEEE VTC2011-Spring, Budapest, Hungary, May 2011.
[9] Y. Matsumoto, K. Tateishi, and K. Higuchi, "Performance evaluations on adaptive PAPR reduction method using null space in MIMO channel for eigenmode massive MIMO-OFDM signals," Proc. APCC2017, Perth, Australia, Dec. 2017.
[10] A. Ivanov, A. Volokhatyi, D. Lakontsev, and D. Yarotsky, "Unused beam reservation for PAPR reduction in massive MIMO system," Proc. IEEE VTC2018-Spring, Porto, Portugal, June 2018.
[11] R. Zayani, H. Shaiek, and D. Roviras, "PAPR-aware massive MIMO-OFDM downlink," IEEE Access, vol.7, pp.25474–25484, Feb. 2019.
[12] S. Shin, N. Nonaka, and K. Higuchi, "User group selection method in multiuser MIMO-OFDM transmission with adaptive PAPR reduction using null space in MIMO channel," Proc. IEEE VTC2020-Fall, Virtual Conference, Nov.-Dec. 2020.
[13] L. Hua, Y. Wang, Z. Lian, Y. Su, and Z. Xie, "Low-complexity PAPR-aware precoding for massive MIMO-OFDM downlink systems," IEEE Wireless Commun. Lett., vol.11, no.7, pp.1339–1343, July 2022.
[14] Y. Sekiguchi, N. Nonaka, and K. Higuchi, "PAPR reduction of OFDM signals using null space in MIMO channel for MIMO amplify-and-forward relay transmission," IEICE Trans. Commun., vol.E105-B, no.9, pp.1078–1086, Sept. 2022.
[15] A. Kakehashi, N. Nonaka, and K. Higuchi, "PAPR reduction using null space in MIMO channel based on signal processing at base station for downlink AF-based relaying MIMO-OFDM signals," Proc. IEEE VTC2022-Fall, London and Beijing, Sept. 2022.
[16] A. Kakehashi, T. Hara, and K. Higuchi, "Base station-driven PAPR reduction method utilizing null space for MIMO-OFDM systems with amplify-and-forward relaying," IEEE Access, vol.12, pp.24714–24724, Feb. 2024.
[17] T. Suzuki, M. Suzuki, Y. Kishiyama, and K. Higuchi, "Complexity-reduced adaptive PAPR reduction method using null space in MIMO channel for MIMO-OFDM signals," IEICE Trans. Commun., vol.E103-B, no.9, pp.1019–1029, Sept. 2020.
[18] L. Yamaguchi, N. Nonaka, and K. Higuchi, "PC-signal-based PAPR reduction using null space in MIMO channel for MIMO-OFDM signals under frequency-selective fading channel," Proc. IEEE VTC2020-Fall, Virtual Conference, Nov.-Dec. 2020.
[19] T. Suzuki, M. Suzuki, and K. Higuchi, "Parallel peak cancellation signal-based PAPR reduction method using null space in MIMO channel for MIMO-OFDM transmission," IEICE Trans. Commun., vol.E104-B, no.5, pp.539–549, May 2021.
[20] T. Hino and O. Muta, "Adaptive peak power cancellation scheme under requirements of ACLR and EVM for MIMO-OFDM systems," Proc. IEEE PIMRC2012, Sydney, Australia, Sept. 2012.
[21] T. Kageyama, O. Muta, and H. Gacanin, "An adaptive peak cancellation method for linear-precoded MIMO-OFDM signals," Proc. IEEE PIMRC2015, Hong Kong, Aug.-Sept. 2015.
[22] J. Saito, N. Nonaka, and K. Higuchi, "PAPR reduction using null space in MIMO channel considering signal power difference among transmitter antennas," Proc. IEEE WCNC2023, Glasgow, Scotland, UK, March 2023.
[23] M. Sharif, M. Gharavi-Alkhansari, and B.H. Khalaj, "On the peak-to-average power of OFDM signals based on oversampling," IEEE Trans. Commun., vol.51, no.1, pp.72–78, Jan. 2003.
[24] H. Ochiai and H. Imai, "Performance analysis of deliberately clipped OFDM signals," IEEE Trans. Commun., vol.50, no.1, pp.89–101, Jan. 2002.

Jun Saito received the B.E. and M.E. degrees from Tokyo University of Science, Noda, Japan in 2022 and 2024, respectively. In 2024, he joined IBM Japan, Ltd. His research interests include wireless communications.

Nobuhide Nonaka received the B.E. and M.E. degrees in electronic engineering from Tokyo University of Science, Japan, in 2013 and 2015, respectively. Since April 2015, he has been with NTT DOCOMO, INC. Since April 2018, he has been engaged in the research of next generation radio access technologies. He received the Young Researcher's Award from the IEICE in 2019. He is a member of the IEICE.

Kenichi Higuchi received the B.E. degree from Waseda University, Tokyo, Japan, in 1994, and received the Dr.Eng. degree from Tohoku University, Sendai, Japan in 2002. In 1994, he joined NTT Mobile Communications Network, Inc. (now, NTT DOCOMO, INC.). While with NTT DOCOMO, INC., he was engaged in the research and standardization of wireless access technologies for wideband DS-CDMA mobile radio, HSPA, LTE, and broadband wireless packet access technologies for systems beyond IMT-2000. In 2007, he joined the faculty of the Tokyo University of Science and currently holds the position of Professor. His current research interests are in the areas of wireless technologies and mobile communication systems, including advanced multiple access such as non-orthogonal multiple access (NOMA), radio resource allocation, inter-cell interference coordination, multiple-antenna transmission techniques, signal processing such as interference cancellation and turbo equalization, and issues related to heterogeneous networks using small cells. He was a co-recipient of the Best Paper Award of the International Symposium on Wireless Personal Multimedia Communications in 2004 and 2007, the Best Paper Award from the IEICE in 2021, a recipient of the Young Researcher's Award from the IEICE in 2003, the 5th YRP Award in 2007, the Prime Minister Invention Prize in 2010, and the Invention Prize of Commissioner of the Japan Patent Office in 2015. He is a senior member of the IEEE.